The Journal of Engineering

The 9th International Conference on Power Electronics, Machines and Drives (PEMD 2018)

IET Journals
The Institution of Engineering and Technology

Design of electromagnetic components for EV battery chargers

eISSN 2051-3305
Received on 22nd June 2018
Accepted on 31st July 2018
doi: 10.1049/joe.2018.8137
www.ietdl.org

Andrea Stratta[1,2] ✉, Paolo Bolognesi[1], Veronica Biagini[2], Matthias Biskoping[2], Fabio Tombelli[3]

[1]*University of Pisa – DESTEC, Italy*
[2]*ABB Corporate Research Center, Germany*
[3]*ABB Power One, Italy*
✉ *E-mail: andrea.stratta1@nottingham.ac.uk*

Abstract: This study focuses on the appropriate design of the inductive elements of the LLC converter based on a typical industrial approach, i.e. assuming to use standard parts available on the market from qualified manufacturers. At first, a methodology to select the passive components is presented, highlighting the difference between the *external inductor solution* and the *magnetically integrated solution*. Secondly the step-by-step procedure used for the design of the high frequency transformer is illustrated. The possibility to integrate the resonant inductors into the HF transformer is then analysed, presenting different solutions. Finally a comparison between a classical and an integrated design is then presented referring to a case study; thus permitting to endow the potential benefits of the integrated solution.

1 Introduction

Battery chargers play a key role in the diffusion of electric vehicles (EV), which represent the best solution for dramatically reducing emissions in urban contexts and pollutants on a global scale. In fact, they are intended to provide controlled power for charging the batteries, balancing at best different key aspects such as battery life preservation, recharge duration, low power losses, minimal distortion and high power factor at the mains size, while also ensuring electrical insulation from the grid for safety purposes. Cost effectiveness, small dimensions and light weight are also important features for such applications, especially when on-board chargers are considered. Several converter topologies have been proposed for EV chargers, [1–3]. Among them, the LLC resonant converter (see Fig. 1) appears very promising for the DC–DC stage which typically carries out both the insulation and voltage/current adaptation functions thanks to the high-frequency transformer included. Several papers focused on the LLC converter have highlighted that the design of the resonant components is crucial in order to achieve high efficiency and robust control, [4–7]. In fact, a proper tuning of the parameters of the resonant tank ensures zero voltage switching (ZVS) operation in broad frequency and power range, resulting in higher efficiency. Thanks to the natural droop of the resonant tank, a frequency-based voltage control can be implemented if the values of the passive elements are appropriate. This paper deals with the design of the magnetic components for a LLC DC/DC converter potentially usable for a battery charger suited for mid-size electrical vehicles. In particular, the possibility to effectively integrate the resonant inductors and the high-frequency transformer is analysed, highlighting the potential benefits.

2 Inductors selection

The converter topology considered in this paper is the LLC converter. As shown in the scheme in Fig. 1, its input stage is composed by a metal-oxide semiconductor field effect transistors (MOSFETs)-based H bridge. Such inverter, fed by the DC voltage source V_{in}, supplies a two-windings high-frequency transformer (HFT) via a series-connected capacitor C_s, which gives rise to a resonant link with the series resonant inductor L_r and the parallel resonant inductor L_p. The output load is supplied by a simple diode rectifier equipped with capacitive tank, which is connected to the secondary winding of HFT. For a correct behaviour of the converter the three passive elements have to be designed: C_s, L_r and L_p. In this section, the resonant converter is analysed using the first harmonic analysis, which means that just the fundamental harmonic is taken into account, and all the other harmonics are considered negligible.

Despite of its simplifying assumptions, this approach is largely used in the literature because it is a good compromise between accuracy and simplicity. In order to achieve ZVS in all load conditions, the critical operating point is the end of the charging process, when the charging current is almost zero. This situation can be approximated with a no-load condition. Basically, the no-load current must be high enough to charge and discharge the drain-to-source capacitance of the MOSFETs, C_{ds}, in a time interval shorter than dead time, T_{dead}:

$$I_{pMin} = \frac{C_{ds} S V_{in}}{T_{dead}} \tag{1}$$

where, V_{in} is the voltage across the resonant tank, S is the number of MOSFETs in the inverter bridge, and T_{dead} is the safety time interval between the switch-off and the following switch-on commands given to the MOSFETs in each leg. In particular, during the no load condition, the only current in the bridge is flowing through the parallel resonant inductor, L_p. At the resonance, C_s and L_r result in a short circuit therefore the voltage across L_p is equal to V_{in}. As a result the maximum value of L_p needed to have I_{pMin} is

$$L_{pMax} = \frac{V_{in}}{2\pi f_r I_{pMin}} \tag{2}$$

Once the value of L_p has been chosen, and since $C_s = 1/((2\pi f_r)^2 L_r)$, the values of L_r can be found by analysing the resonant tank voltage transfer function. A graphical analysis of the transfer

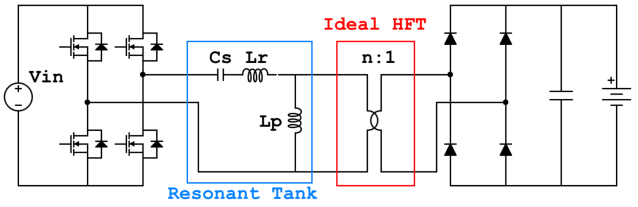

Fig. 1 *LLC resonant converter topology with ideal HFT*

Table 1 Resonant converter specifications for case study

P_{nom} = 10 kW	V_1 = 700 V ÷ 900 V
f_{nom} = 100 kHz	V_2 = 320 ÷ 440 V

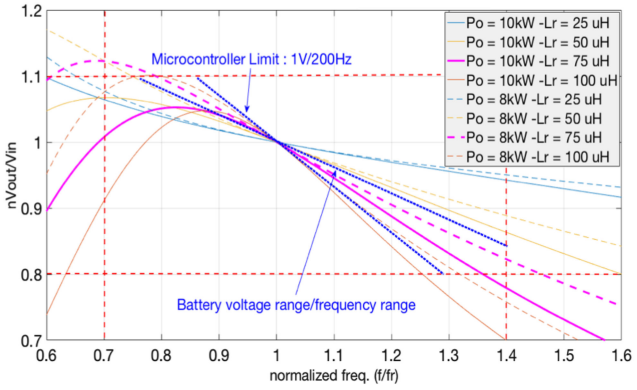

Fig. 2 *Transfer function with limits*

function is sufficient to understand if the resonant tank can fulfill its main tasks:

1. To have ZVS the current must lag the voltage. That means that the equivalent impedance must behave as an inductor, resulting in magnitude decreasing with the frequency.
2. In order to implement a voltage control based on the variation of switching frequency, the function linking this quantity to the output/input voltage ratio must be monotonic in the considered operation interval. To achieve this condition, the curve of the transfer function must be monotonic in the operative frequency interval.
3. The maximum slope of the *V–f* curve is due to the micro-controller frequency resolution, Δf (f), and the requested sensitivity of the voltage control, ΔV_c. In fact, the micro-controller used for the closed loop control is not capable of increasing the frequency continuously, therefore the normalised slope of the transfer function must not be greater than the ratio $\Delta V_c/\Delta f(f)$.
4. The minimum slope of the resonant tank droop is defined both by the voltage interval and the frequency interval in which the controller should operate. The voltage range is due to the charging profile of the battery.

Based on these assumptions, a good value for L_r can be estimated looking at the transfer function graph. Different transfer functions associated to different value of L_r can be plotted. When the transfer function is in between the maximum and minimum slope constraints, the value of L_r is appropriate.

To give an example, a case study has been analysed, its specifications are listed in Table 1. Using the procedure explained above, the maximum value of L_p is calculated, and it is equal to 300 µH. The transfer function is then plotted with this value of L_p and varying L_r, see Fig. 2. Looking at this graph, it is clear that L_r = 75 µH is an appropriate value for this case study. As a result, the value of the resonant capacitor is C_s = 38.5 nF.

3 External inductors and magnetically integrated solution

The first possible approach in the design of the magnetic components for LLC converters consists in designing a transformer, then calculating its leakage and magnetising inductances and subsequently introducing external inductors to match the converter requirements, when the values of the inherent parameters of the transformer are lower than required; later on this approach will be called *external inductor solution*. The other approach is the *magnetically integrated solution*, [8–10]. The magnetic integration is the option to exploit the magnetising and leakage inductances of the transformer in order to avoid the use of any external inductors in the converter. The potential benefits of such solution consist in the reduction of the overall size, weight, cost and losses of the magnetic components. In the next sections, the two approaches are presented and finally a comparison based on the case study above introduced is made.

4 External inductors solution

In this work, the *external inductors solution* has been developed following three steps: *high frequency transformer analytical design*, *finite element model* (*FEM*) *validation*, and *external inductors design*.

4.1 High-frequency transformer analytical design

The preliminary design of the high frequency transformer is carried out by means of an analytical function developed in MATLAB. Thanks to the analytical function it is possible to analyse different transformers and subsequently select the one with the highest efficiency, taking material cost and overall dimensions into account as well.

Libraries creation: The final goal of the analytic function is to be a user-friendly tool to analyse transformers made of different combinations of core materials, core dimensions, wires type and number of turns. To do so three main libraries have been created:

- *Core materials library*: It collects the most promising materials for this application. Different kinds of ferrite and nanocrstallyne materials from three major manufacturers (*Ferroxcube*, *Vaccumshmelze* and *Hitachi – Metals*) are included. For each material, Steinmetz coefficients and density are defined.
- *Core shapes library*: This library collects ferrite pot cores and 2E cores, and nanocrystalline 4C cores. Each core shape is stored in several standard dimensions.
- *Litz wires library*: It collects different Litz wires from a major manufacturer. External diameter, strand diameter, cross section and copper effective section are defined for each Litz wire.

Geometric calculation: It should be noted that primary and secondary windings are considered to be concentric and wrapped around the central column of the core. Multiple layers for each winding may be used. The minimum insulation distance between coils and between coils and core is calculated considering air, in the worst possible condition, as the insulator:

$$d_{iso} = \frac{V_{in}\ \mathrm{V}}{1000,\ \mathrm{V/mm}} \tag{3}$$

Combining the information coming from the *Core shapes library* and *Litz wires library* together with the number of turns it is possible to understand if the windings fit in the core window. If the windings fit inside the window, the function proceeds with the calculation of the wires length and the copper mass.

Core loss calculation: In order to estimate the core losses, the average value across the core of the peak flux density value B_m is calculated. Considering a periodic voltage applied to a coil the peak value of B_m is [11]:

$$B_m = \frac{V_{avg}}{4 f A_{eff} N_1} \tag{4}$$

where V_{avg} is the average value of the voltage applied to the coil calculated on a half period, A_{eff} is the effective cross section of the core and N_1 is the number of turns. Once B_m is known, several approaches can be used for the core losses calculation. Since here the aim is to develop an analytic function, a compromise between accuracy and simplicity has been done. On this basis, and considering that with an LLC converter the voltage waveforms applied to the transformer windings are almost sinusoidal, the

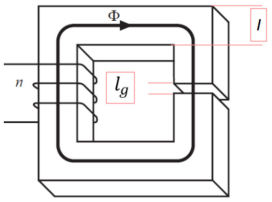

Fig. 3 *Inductor using a C-core*

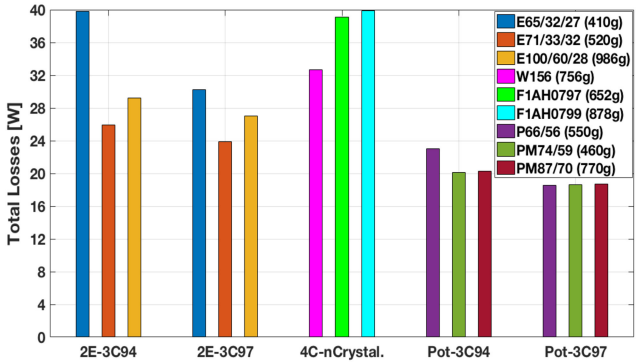

Fig. 4 *Best combinations from the library for HFT*

Table 2 Analytical results vs. FEM results

Core size	Core losses		Copper losses	
	An., W	FEM, W	An., W	PE_{mag}, W
E71/33/32-3C94	6.33	6.51	19.60	13.35
E71/33/32-3C97	6.44	6.63	17.43	11.18
PM74/59-3C94	5.79	6.71	14.35	11.12
PM74/59-3C94	4.24	5.06	14.35	11.12

common Steinmetz equation is used [12]. Thanks to this equation the average value of the core losses can be calculated:

$$P_c = (k f^{\alpha} B_m^{\beta})\mathrm{Vol} \tag{5}$$

where Vol is the core volume and k, α β, are the Steinmetz coefficients, available from manufacturers and also included in the materials library.

Copper loss calculation: In high-frequency devices, the losses associated with windings are considerably increased by two phenomena, skin effect and proximity effect. In order to reduce these effects, Litz wires are used. Due to the complexity of Litz wires, every analytical approach uses several simplifications and approximations. In order to have a better estimation of the copper losses two different approaches have been implemented in the MATLAB procedure get ready: Sullivan approach [13] and Tourkhani approach [14]. These two models consider the single strand of the Litz wire as a conductive cylinder exposed to a transverse magnetic field. The first model considers only the *external* field, whereas the second model takes into account the conductor *internal* field as well.

4.2 FEM validation

The electromagnetic FEM analysis software *AnsysMaxwell*® has been used in this project to analyse and simulate the transformers behaviour. In order to have an estimation of the total losses, two different simulations are needed:

- *Magnetic transient simulation*: It consists of an open-circuit test under sinusoidal nominal voltage excitation. Through this test both core losses and inductances are calculated.
- *Simulation with PEmag*: Since it is not possible to perform FEM simulations on Litz wires with a high number of strands, an additional tool of *Maxwell*® has been used, PEmag. Thanks to this tool it is possible to have an analytical estimation of the AC resistance of transformers windings made of Litz wires [15].

The whole 3D model of the transformer is built directly in *Maxwell*® In order to simplify the simulation, for the magnetic transient analysis the windings are modelled as a unique pseudo cylindrical body, and all the symmetries are exploited allowing to analyse just one eighth of the whole transformer.

4.3 External inductors design

The analytic design of the inductors is based on a gapped C-core shape, see Fig. 3, but the same procedure can be used for gapped double E-cores. The first hypothesis is to neglect the reluctance of the core compared with the reluctance of the gap, and this can be done just if $l_g \gg l_{core}/\mu_{core}\mu_0$.

Since the magnetic field inside the core is negligible compared with the magnetic field in the gap, the magnetic energy is considered to be stored just in the air gap volume. The second hypothesis is that the length of the gap, l_g, is much smaller than the cross section side dimension, l. Thanks to this hypothesis, the field is considered to be perpendicular to the core surfaces in the whole gap, which means that the volume of air, Vol_{air}, in which the energy can be calculated is a brick box

$$E = \frac{1}{2}LI_{max}^2 = \frac{\mathrm{Vol}_{air}B_{max}^2}{2\mu_0} = \frac{l^2 l_g B_{max}^2}{2\mu_0} \tag{6}$$

where L is value of the inductance, I_{max} is the maximum value of the current flowing in the winding, and B_{max} is the maximum value of the flux density. Neglecting the m.m.f. drop in the core, the Ampere law applied on a closed loop which links the windings results in

$$nI_{max} = \frac{B_{max}}{\mu_0} l_g \tag{7}$$

where n is the number of turns of the winding. Assuming to fix γ the ratio between the cross section's side dimension and the gap, by combining (6) and (7) the three equations used for the inductors design can be derived:

$$l = l_g\gamma, \quad l_g = \sqrt[3]{\frac{LI_{max}^2\mu_0}{B_{max}^2\gamma^2}}, \quad n = \sqrt[3]{\frac{LB_{max}}{\mu_0^2 I_{max}\gamma^2}} \tag{8}$$

4.4 Case study

In order to design an appropriate HFT for the case study presented in Section 2, the analytic function has been used to analyse different combinations of elements. For each combination of core material, core shape and Litz wires the number of turns corresponding to the maximum efficiency has been found.

In Fig. 4, the best solutions are shown, in particular the core materials are 3C94 and 3C97 (power ferrite from *Ferroxcube*) and Vitroperm500F (nanocrystallyne from *Vacumshmelze*) and Finemet-3M (nanocrystallyne from *HitachiMetals*). They have been divided in five different groups, in each group there is the same material and the same core shape in three different dimensions. From this graph it is clear that, in this frequency range, nanocrystalline materials are not competitive with power ferrite. For each ferrite group, the best core dimension can be found: for the E-cores E71/33/32 and for pot-cores PM74/59 both in 3C94 and 3C97. These four transformers are then modeled and analysed using *Maxwell*®; thus permitting a comparison between analytical and FEM results (see Table 2).

The average error for the core losses estimation is 6%, while for the copper losses it is 30%. However, it must be noted that for the estimation of the AC resistance Maxwell® is using an analytic equation too. Therefore, the analytical procedure get ready can be considered as basically validated, at least for the core losses calculation. Regarding the copper losses, the larger error is

Table 3 Best transformers: efficiency and inductances

Core size	Efficiency, %	Magnetic inductance, mH	Leakage inductance, μH
E71/33/32-3C94	99.74	13.05	$L_{lk,1} = 9.7$
E71/33/32-3C97	99.76	12.88	$L_{lk,1} = 8$
PM74/59-3C94	99.8	12.41	$L_{lk,1} = 13.7$
PM74/59-3C94	99.82	15.51	$L_{lk,1} = 6.3$

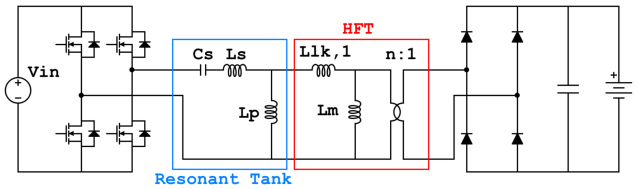

Fig. 5 *LLC converter topology with external inductors*

Table 4 Series and parallel inductors mass and losses

	Mass, g	Copper loss, W	Core loss, W
series inductor	940	8	35
parallel inductor	80	1	3

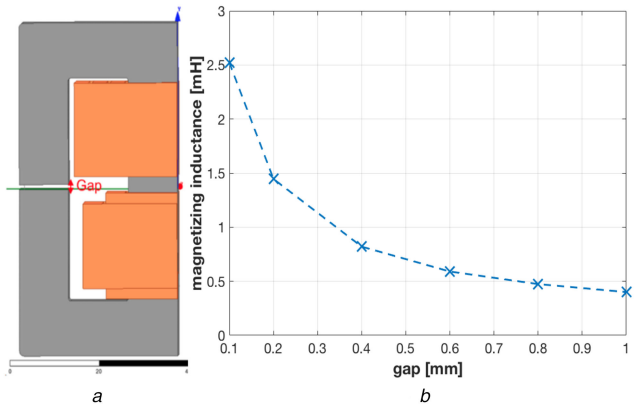

Fig. 6 *2E-core with non-concentric windings and gaps*
(a) Model, ***(b)*** Magnetising inductance vs. gap width

Table 5 Analytical results vs. FEM results

Losses, W	Mass, g	L series, μH	L parallel, μH
HFT + ext. ind.			
HFT: 26	HFT: 700	75	300
Ind: 47	Ind: 1020		
tot: 73	*tot*: 1720		
Mag. int.			
44	700	60	300

motivated by the difficulty faced in the modelling of Litz wires: actually, no FEM software is presently able to effectively analyse in detail the behaviour of wires including a large number of strands. Therefore, the use of different analytical approaches with different assumptions can lead to slightly different results.

The values of the inductances of these four transformers are another important result obtained by FE simulations, and they are shown in Table 3. Looking carefully at this table it is interesting to note that (see Fig. 5):

1. The values of magnetising inductances are so high with respect to the target values that these elements can be neglected: therefore an external parallel resonant inductor having inductance value (L_p) equal to the target must be used in all of the four considered solutions.
2. On the opposite, the values of leakage inductances are not negligible with respect to the target value. Therefore, an external series resonant inductor (L_s) must be introduced whose value Ls has to be chosen keeping into account the leakage inductance.

Therefore, on the basis of the analysis performed in Section 2, in order to use the first transformer (E71/33/32-3C94) in the LLC resonant converter, the external series resonant inductor must be $L_s = 60$ μH and the external parallel inductor must be $L_p = 300$ μH. Using the equation presented in the latter paragraph, it is possible to design the two external inductors made of ferrite 3C94, their main characteristics are reported in Table 4.

5 Magnetically integrated solution

Several magnetically integrated solutions have been thoroughly investigated, among them two specific transformer layouts proved to permit both to match the target inductance values and to reduce weight, dimensions and losses. The first transformer solution features a relatively conventional layout, including gaps and using non-concentric windings. The second transformer layout presents many novelties with respect to other solutions available on the market, therefore it was submitted to the ABB intellectual property office for possible patenting, and it cannot be presented in this paper.

5.1 2E-core with non-concentric windings and gaps

In the design proposed in Section 3, the windings were concentric, resulting in low leakage flux. The first solution to increase the leakage inductance consists in piling up the two windings as shown in Fig. 6*a*. Thanks to this modification, the leakage inductance is increased from 10 μH (transformer with concentric winding) up to 60 μH. Moreover to solve the problem of the high value of magnetising inductance, gaps can be added in the lateral columns, Fig. 6*a*. In fact, the introduction of gaps increases the reluctance of the linked flux path, resulting in a smaller magnetising inductance. In particular, varying the gap length from 0.1 to 1 mm the magnetising inductance can be reduced from 2.5 mH down to 300 μH, as shown in Fig. 6*b*. The leakage inductance turns out to be practically unaffected by the gap variation. However, referring to the values selected in Section 2, the leakage inductance does not reach the target of 70 μH. As a consequence, the slope of the natural droop is flatter and therefore the converter will operate in a wider frequency range. Apart from the most promising solution that cannot be illustrated in this paper as it is presently considered for patenting, the above structure turned out to be the second most suited one for the considered case study. Therefore, transient FEM simulations have been performed in order to determinate the total losses. The results of these simulations are summarized in Table 5.

6 Comparison of analysed solutions

A comparison of the main features of the selected configurations for the external and integrated solutions is presented in Table 5. As expected, the magnetically integrated solution results in a reduction of weights, from 1.718 kg to 700 g (60% of mass reduction). Thanks to a reduced use of materials, the converter can be more compact and cost effective. In terms of total losses, the magnetically integrated solution is again better than the other other: in fact, they drop from 73 W down to 44 W, with a remarkable reduction by about 40%. The only drawback of this magnetically integrated solution is the practical difficulty to tune the leakage inductance. In fact, thanks to the piled-up layout of the windings it is possible to achieve high leakage inductance, but the design is missing a dedicated adjustable parameter permitting to achieve a broad independent tuning of leakage inductance.

7 Conclusions

The LLC topology represents an interesting solution for DC/DC insulated resonant converters. An automated procedure for the selection of appropriate values for the resonant components was

presented. An analytic approach was used for the transformer design. In the end, for this case study the design procedure provided four candidates. Using *AnsysMaxwell*® 3D FEM models of the four promising candidates were implemented. Thanks to the simulation results the analytical procedure was considered validated, at least for the core loss calculation. In terms of leakage and magnetising inductances, the four transformers did not match the converter requirements by themselves. For this reason, a series and a parallel inductor have been designed. The option of adjusting the transformer structure and design to meet also the inductance requirements was then investigated. Among the investigated solutions, the most promising is presently under patenting, whereas the second one features a non-concentric deployment of the windings and the introduction of appropriate gaps in the lateral columns of the core, thus ensuring appropriate values of leakage and magnetising inductances. Finally, the second solution was compared to the one using external inductances in terms of size, weight and losses, confirming the potential benefits deriving from magnetic integration.

8 References

[1] Yilmaz, M., Krein, P.T.: 'Review of battery charger topologies, charging power levels, and infrastructure for plug-in electric and hybrid vehicles', *IEEE Trans. Power Electron.*, 2013, **28**, (5), pp. 2151–2169

[2] Khaligh, A., Dusmez, S.: 'Comprehensive topological analysis of conductive and inductive charging solutions for plug-in electric vehicles', *IEEE Trans. Power Veh. Electron.*, 2012, **61**, (8), pp. 3475–3489

[3] Williamson, S.S., Rathore, A.K.: 'Industrial electronics for electric transportation: current state-of-the-art and future challenges', *IEEE Trans. Ind. Electron.*, 2015, **62**, (5), pp. 3021–3032

[4] Shafiei, N., Arefifar, S.A., Saket, M.A.*, et al.*: 'High efficiency LLC converter design for universal battery chargers'. Applied Power Electronics Conf. and Exposition (APEC), Long Beach USA, 2016

[5] Deng, J., Li, S., Hu, S.*, et al.*: 'Design methodology of LLC resonant converters for electric vehicle battery chargers', *IEEE Trans. Veh. Technol.*, 2014, **63**, (4), pp. 1581–1592

[6] Ivensky, G., Bronshtein, S., Abramovitz, A.: 'Approximate analysis of resonant LLC dc–dc converter', *IEEE Trans. Power Electron.*, 2011, **26**, (11), pp. 3274–3284

[7] Musavi, F., Craciun, M., Gautam, D.S.*, et al.*: 'An LLC resonant dc–dc converter for wide output voltage range battery charging applications', *IEEE Trans. Power Electron.*, 2013, **28**, (12), pp. 5374–5445

[8] Chen M, L.Q., Chen, B.: 'The integrated LLC resonant converter using center-tapped transformer for on-board EV charger'. Energy Conversion Congress and Exposition (ECCE), Montreal, Canada, 2015

[9] Cougo, B., Kolar, J.: 'Integration of leakage inductance in tape wound core transformers for dual active bridge converters'. Int. Conf. of Integrated Power Electronics Systems (CIPS), Nuremberg, Germany, 2012

[10] Zhang, J., Ouyang, Z., Duffy, M.C.*, et al.*: 'Leakage inductance calculation for planar transformers with a magnetic shunt', *IEEE Trans. Ind. Appl.*, 2014, **50**, (6), pp. 4107–4112

[11] Ortiz, G., Biela, J., Kolar, J.: 'Optimized design of medium frequency transformers with high isolation requirements'. 36th Annual Conf. of IEEE Industrial Electronics Society (IECON 2010), Glendale, USA, 2010

[12] Venkatachalam, K., Sullivan, C.R., Abdallah, T.*, et al.*: 'Accurate prediction of ferrite core loss with nonsinusoidal waveforms using only Steinmetz parameters'. Proc. of IEEE Workshop on Computers in Power Electronics, Mayaguez, Puerto Rico, USA, 2002

[13] Sullivan, C.R.: 'Optimal choice for number of strands in a Litz-wire transformer winding', *IEEE Trans. Power Electron.*, 1999, **14**, (2), pp. 283–291

[14] Tourkhani, F., Viarouge, P.: 'Accurate analytical model of winding losses in round Litz wire windings', *IEEE Trans. Magnetics*, 2001, **37**, (1), pp. 538–543

[15] Lotfi, W., Lee, F.C.: 'A high frequency model for Litz wire for switch-mode magnetics'. Proc. IEEE 28th Industry Applications Conf. (IAS Annual Meeting), Toronto, Canada, 1993, **vol. 2**, pp. 1169–1175